An online method to simultaneously identify the parameters and estimate states for lithium ion batteries

Qianqian Wang [a, c], Jianqiang Kang [a, c, *], Zuxian Tan [b], Maji Luo [a, c]

[a] Hubei Key Laboratory of Advanced Technology for Automotive Components, Wuhan University of Technology, Wuhan 430070, PR China
[b] Shenzhen Pengcheng New Energy Technology Co., LTD, Shenzhen 518102, PR China
[c] Hubei Collaborative Innovation Center for Automotive Components Technology, Wuhan University of Technology, Wuhan 430070, PR China

ARTICLE INFO

ABSTRACT

Currently, state of charge (SOC) estimation on the basis of Kalman filter (KF) is realized to be applied online, but the parameters of the battery model that is implanted in KF are commonly identified offline. The offline identification is not only a time-consumed process but also provides the inaccurate results. Considering the complex and changeable operating conditions of batteries employed in electric vehicles, the parameters are also varied in fact and need to be identified online, by which the real state of the battery is reflected. In this study, the online identification of parameters and estimation of SOC are fulfilled simultaneously by using a novel algorithm named dual unscented Kalman filter (DUKF). Results show that the parameter identification on the basis of the DUKF accurately simulates the dynamic performance of the terminal voltage. By using the proposed algorithm and under three different operating conditions, the state of the battery is effectively estimated. The maximum error of SOC estimation is less than 3%, which is better than the results by using the extend Kalman filter (EKF) and unscented Kalman filter (UKF). Furthermore, the online identification of parameters that are changeable and related to the fading state of the battery, enables the state of health (SOH) to be estimated online.

© 2018 Elsevier Ltd. All rights reserved.

1. Introduction

Currently, the contradiction between automobiles and energy supply, environmental protection as well as other social carrying capacity has become increasingly prominent with the expansion of the car ownership [1]. Rational distribution of electric vehicles as the representative of the new energy automotive industry has become an important direction of the future economic development. As the core component of electric vehicles, the power battery is the key factor that determines the healthy and rapid development of electric vehicles. Because of its high energy density, long cycle life, low self-discharge rate, no memory effect and green environmental protection, the lithium-ion battery has become the first choice for electric vehicles. Although lots of progress and achievements have been made in research and industrial application of lithium-ion batteries, the problem of safety and life still restricts the popularity of electric vehicles and large-scale

applications. This case requires an accurate battery management system (BMS) to control the batteries in real time, especially to estimate the actual state of charge (SOC) [2]. The real time SOC is the basis for the BMS to obtain energy, power and safety information from the battery and feedback to the vehicle. Therefore, the accurate estimation of SOC has a significant impact on the vehicle's dynamic performance and safety.

The SOC estimation methods are mainly consisted of the current integration [3], the open circuit voltage [4,5], the black-box model based method [6,7] and the model based filtering method [8–11]. The current integration method is easy to calculation but have no automatic error correction function which causes a large number of error accumulations. The open circuit voltage method requires a lot of time and energy for measurement. The black-box model based methods, such as support vector regression, fuzzy control and neural networks need sufficient offline training data, thus they are hard to achieve online estimation. For a real application, the model based filtering method seems to be the most promising, especially the Kalman filter-based methods, such as extend Kalman filter (EKF) [12–14], sigma points Kaman filter (SPKF) [15–17], and the interacting multiple model (IMM) Kalman filter [18]. This method is believed to meet the common requirements of the BMS, such as the real-time response performance, low-cost hardware, high accuracy

---

* Corresponding author. Hubei Key Laboratory of Advanced Technology for Automotive Components, Wuhan University of Technology, Wuhan 430070, PR China.

E-mail address: kjqiang@sohu.com (J. Kang).

etc.

The accurate identification of dynamic battery parameters is the premise that ensures the safe and reliable operation of a lithium-ion battery system. At present, the parameters are commonly identified by HPPC test that is an offline method. The offline identification is not only a time-consumed process but also provides the inaccurate results, for the detection quantity is accompanied by the uncertainty noise signal in the process of modeling. The errors generated by the noise in real time can be compensated if parameter identification is carried out by an online method. The Kalman filtering has been widely used in online parameters identification, providing a direct solution of random noise [33,34]. The random noise is filtered out to obtain the exact space state value by treatment of the measured data. Lately, using the Kaman-based methods or observers to estimate parameters and states seems to be very promising [26]. To estimate the state and parameters of the system simultaneously, joint Kalman filtering (JKF) [19–22] or dual Kalman filtering (DKF) [23–33] can be employed. The JKF algorithm considers the online identified parameters as the system state, and thus needs to expand the dimension of the original system state variables, may leading to high-dimensional vectors and complex matrix operations. The DKF algorithm uses two independent Kalman filters to estimate the system state and to identify the parameters, respectively, and thereby avoiding the increase of dimensionality that leads to the complicated calculation. Therefore, the DKF algorithm is more widely used. Dave Andre [26] introduced a dual filter consisting of a standard Kalman filter and an Unscented Kalman filter to estimate the parameters and SOC. Despite of this method with good results, the capacitance was treated as a constant so that a lot of time is needed to off-line measure the specific capacitance and thus is difficult to achieve online estimation. Jonghoon Kim [32] proposed an algorithm based on dual extended Kalman filter (DEKF) to estimate SOC/SOH and B. S. Bhangu [33] used Kalman filter to estimate SOC and extended Kalman filter to estimate SOH. Both the abovementioned methods used extended Kalman filter for dimensionality reduction. However, the extended Kalman filter leads into derivative calculation in the process of linearizing, increasing the operating load of Micro Control Unit (MCU). The specific literature comparison is shown in Table 1.

After review of the previous literatures, we find that some parameters were assumed as constants when SOC estimation was implemented. The assumed parameters not only cause the long time data calibration but also reduce the precision. Some papers only partially identified the model parameters. And some estimation algorithms have the disadvantages of low accuracy, large

dimensions, and high complexity. Therefore, a better approach is to find a suitable method with high efficiency and accuracy, realizing simultaneously the estimation of the states and the identification of all parameters. To overcome the above-mentioned shortcomings, it is necessary to propose a new algorithm.

In view of the above deficiencies, a dual Unscented Kalman filter (DUKF) is proposed in this study to fulfill online the parameters identification and the SOC estimation on the basis of the dual polarization (DP) model that considers both electrochemical polarization and concentration polarization. For the state estimation, the algorithm takes the real time change of parameters into account, compensates the noise signals during the operation and avoids the influence of the ambient factors in practice, so the accuracy and efficiency of the method are better than that of EKF and UKF. In terms of parameters online identification, the DUKF algorithm used in this study can estimate not only SOC but also SOH in real time, since the changeable parameters are related to the fading state of the battery.
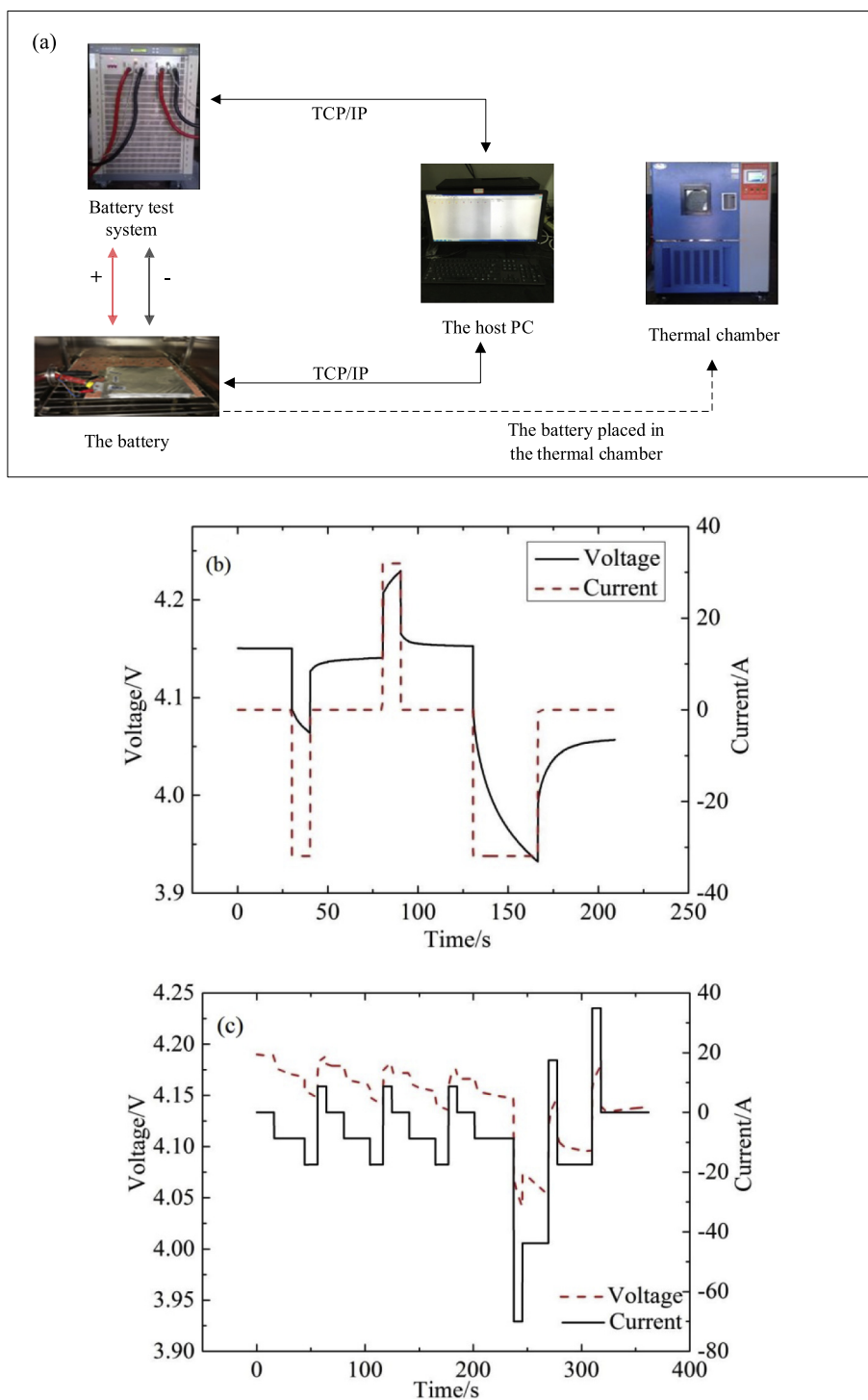
2. Experiments

Experimental studies were conducted on a graphite/$LiNi_xCo_yMn_{1-x-y}O_2$ battery that had a rated capacity of 35 Ah and a nominal voltage of 3.7 V. As shown in Fig. 1(a), the experimental bench comprised a Neware battery test system (BST 7.5.3 Newaresles) for battery charging and discharging, a host PC (Intel(R) Core(TM) i7-4770 CPU@3.40 GHz) for signal acquisition, and a thermal chamber (GDJS-150 WuXi Youlian Ltd.) for temperature control. To ensure the consistency of the measurement conditions, the cell was placed in a constant temperature of 25 °C during the whole test. The battery test system acquisition module has temperature sensors to collect the surface temperature of the battery. Although the collected data show a slight increase in temperature, it can be ignored since the battery performance is changed slightly with a little increase of the temperature.

The experiment projects were designed to test the basic performance and dynamic adaptability. The entire tests include a static capacity test, a constant current discharge (CCD) test, a hybrid pulse power characterization (HPPC) test referred to Ref. [37] and a dynamic stress test (DST) referred to Ref. [35]. The HPPC test shown in Fig. 1(b) can not only be used to realize the offline battery parameters identification, but also be regarded as an operating condition. The DST test shown in Fig. 1(c) is mainly used to test the dynamic performance of the battery and simulate the running condition of the vehicle with variable power. Before the DST test the peak power

Table 1
Literatures comparison.

	Algorithm	Parameter identification	State estimation	Advantage or Disadvantage	Reference
1	KF-UKF	Partial parameters	SOC and SOH	The polarization capacitances are treated as constants.	[26]
2	DEKF	Partial parameters	SOC and SOH	This paper only studied the online changes of parameter R_{Diff}.	[32]
3	KF-EKF	All parameters	SOC and SOH	The KF algorithm is only suitable for handling linear problems, and the EKF algorithm can only achieve first-order estimation accuracy.	[33]
4	EKF-UKF	All parameters	SOC and SOH	The EKF algorithm uses a first-order Taylor expansion to deal with nonlinear problems. Although this method can linearize the problem, it ignores the discrete distribution of random variables.	[30]
5	JEKF	All parameters	SOC and SOH	The joint Kalman filter algorithm causes the dimension of the state variable to increase and the amount of calculation is larger; The EKF algorithm only achieves first-order accuracy, which easily leads to loss of precision.	[19]
6	JUKF	All parameters	SOC and SOH	The joint Kalman filter algorithm causes the dimension of the state variable to increase and the amount of calculation is larger.	[20]
7	DUKF	Partial parameters	SOH	This paper only studied the online changes of internal resistance.	[39]
8	DUKF	All parameters	SOC and SOH	The DUKF algorithm used in this study has superior theoretical advantages.	This study

Fig. 1. (a) The experimental bench; (b) The sampling curve of current and voltage under the HPPC test; (c) The sampling curve of current and voltage under the DST test.

is need to tested first.

3. Introduction of the battery model and the parameters identification

3.1. The equivalent circuit model

The equivalent circuit models are widely employed in BMS because of the simple structure and the availability in an online case. The commonly used equivalent circuit models mainly include the Thevenin model, the PNGV model and the DP model. Among them, the DP model shown in Fig. 2 is selected in this study because we have proved that it has the best dynamic performance, providing the most accurate state estimation and meeting the requirements of BMS [36].

In Fig. 2, U_{ocv} represents the open circuit voltage of the battery. It corresponds to a specific SOC value and has a very strong nonlinear relationship with the SOC. The U_{ocv}-SOC curve of the specified
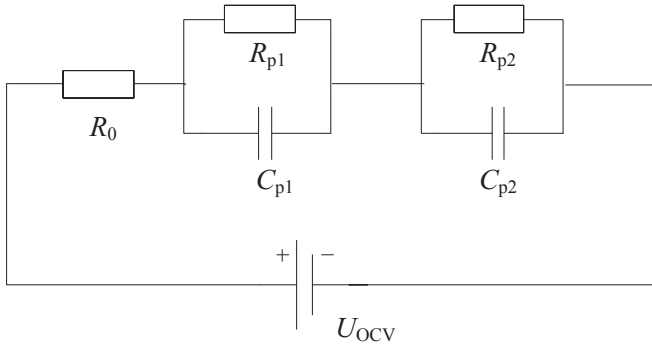
Fig. 2. DP model structure.

battery can be obtained by look-up table. I is the load current, U_L is the terminal voltage, R_0 is the internal resistance, C_{p1} and R_{p1} are the capacitance and resistance of electrochemical polarization respectively, C_{p2} and R_{p2} are the capacitance and the resistance of concentration polarization respectively. R_{p1}, C_{p1} and R_{p2}, C_{p2} constitute two RC parallel loops are used to simulate polarization effects. According to Kirchhoff's law of voltage and current, the equation is as follows [14]:

$$\begin{cases} U_L = U_{ocv}(SOC) - IR_0 - U_{p1} - U_{p2} \\ \dot{U}_{P1} = -\dfrac{1}{C_{P1}R_{P1}}U_{P1} + \dfrac{1}{C_{P1}}I \\ \dot{U}_{P2} = -\dfrac{1}{C_{P2}R_{P2}}U_{P2} + \dfrac{1}{C_{P2}}I \end{cases} \tag{1}$$

3.2. Off-line parameters identification

To obtain the model parameters, the method used in general is the HPPC test. The sampling curve of current and voltage under the HPPC test is shown in Fig. 1. The U_{ocv} is an important parameter in the battery model and the relationship between the U_{ocv} and SOC can be calculated referred to [37]. The U_{ocv}-SOC relationship curve is shown in Fig. 3. The circle represents the value of the U_{ocv} corresponding to each SOC point. The black solid line represents the fitting curve of U_{ocv}-SOC. The R-square is characterized by the change of the data to represent the good or bad of a fitting. The normal value range of the R-square is 0–1 and the closer to 1 the better for curve fitting.

R_0 can be calculated by the voltage difference when the current turn-on instant. The calculation formula for the discharge direction according to Fig. 4 is shown as follows:

$$R_0 = \frac{\Delta U_{AB} + \Delta U_{DC}}{2I} \tag{2}$$

ΔU_{AB} is the voltage drop in AB segment and ΔU_{DC} is the voltage recovery in DC segment. Then, the polarization parameters are fitted by double exponential fitting by analyzing the BC and DE segments for the discharge direction. The DE segment is analyzed first, the initial voltages of the C_{p1} and C_{p2} is $U_1(0)$ and $U_2(0)$, respectively. The mathematical relation of the terminal voltage in the DE segment is as follows:

$$U_L(t) = U_{ocv} - U_1(0)e^{-t/\tau_1} - U_2(0)e^{-t/\tau_2} \tag{3}$$

$$\begin{aligned} \tau_1 &= R_{p1}C_{p1} \\ \tau_2 &= R_{p2}C_{p2} \end{aligned} \tag{4}$$
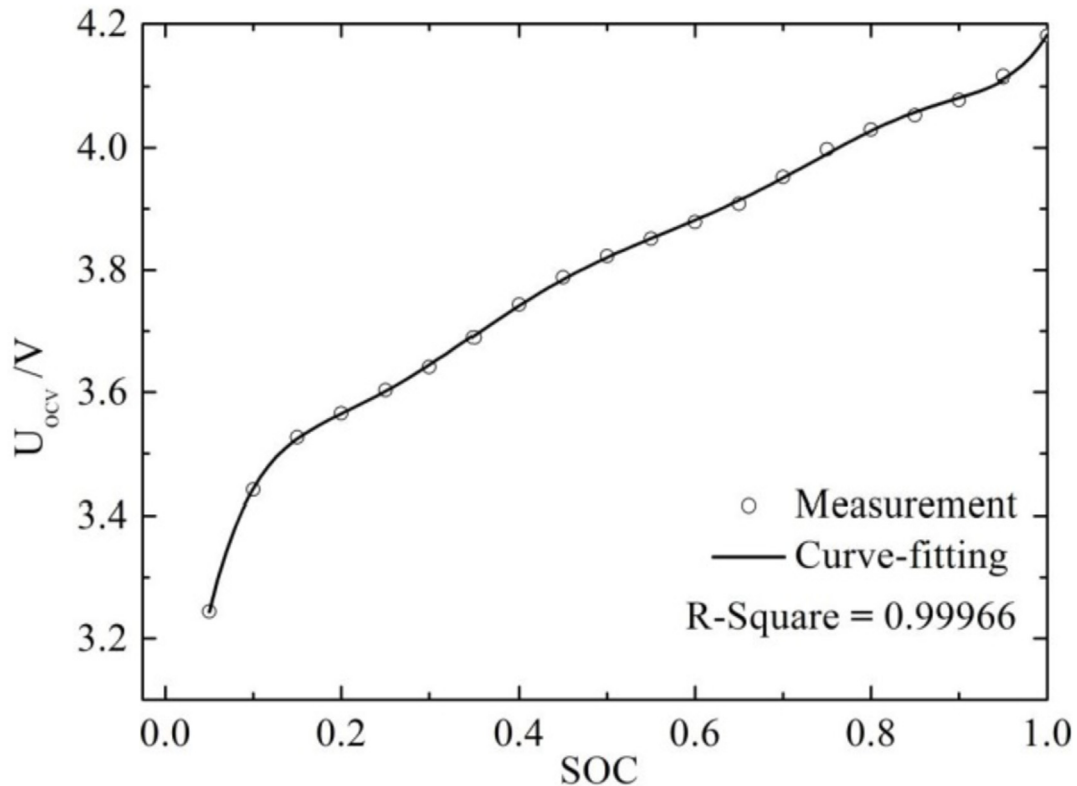
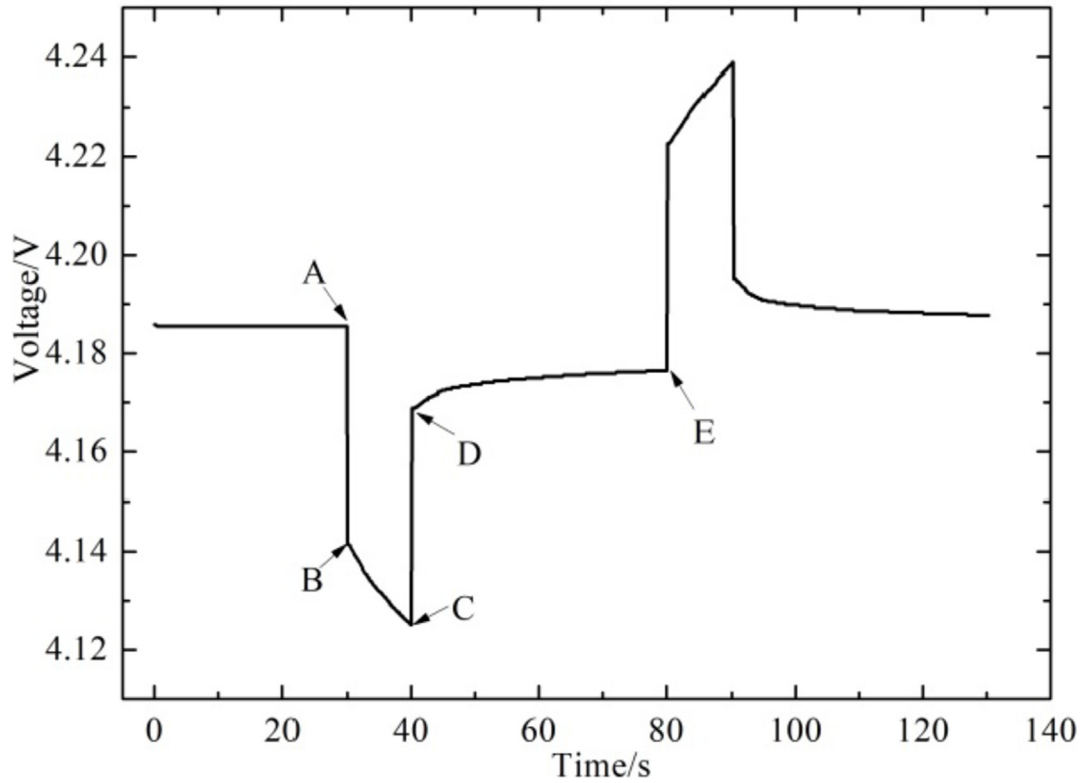**Fig. 3.** The curve of U_{ocv}-SOC under the HPPC test.

Fig. 4. The voltage change of HPPC test.

For the BC segment, the pulse constant current discharge current is I, the zero state response of the two RC circuits can be expressed as:

$$U_1(t_c) = I \times R_{P1}\left(1 - e^{-t_c/\tau_1}\right) \quad U_2(t_c) = I \times R_{P2}\left(1 - e^{-t_c/\tau_2}\right) \quad (5)$$

$R_{p1}, \tau_1, R_{p2}, \tau_2$ can be identified through BC and DE segments, and then C_{p1}, C_{p2} can be calculated as well according to equation (4).

4. SOC estimation methods

4.1. An introduction to EKF and UKF

The EKF algorithm shown in Table 2 has been widely used to estimate SOC nowadays. However, it still has some insurmountable limitations, for example the precision missing of the higher order when solving the nonlinear problem by the first order Taylor expansion equation. To overcome this deficiency, Julier et al. [38] proposed unscented Kalman filtering on the basis of sampling principle of UT transform. The basic idea of unscented Kalman filtering is concisely summarized as: a certain number of sampling points (sigma points) with the same mean and covariance of the system state distribution are selected, and then the posterior mean and covariance of the system state are calculated based on the results of the nonlinear transformation of the sigma points. The summary of UKF algorithm is shown as follows:

Tables 2 and 3 show the basic equations based on two kinds of Kalman algorithms. As long as the initial state variable $\hat{x}_{(0)}$ and the initial covariance matrix $P_{(0)}$ are given, the state variable $\hat{x}_k$ can be calculated by recursion on the basis of the observation quantity z_k. Where the u is the control input vector, w is the system noise, v is the observation noise, Q is the system noise covariance

Table 2
Summary of EKF algorithm.

The state equation (6) and the observation equation (7) of the nonlinear discrete system:

$$x_k = f(x_{k-1}, u_{k-1}) + \omega_{k-1} \quad (6)$$

$$z_k = h(x_k, u_k) + v_k \quad (7)$$

Step 1 Initialization: For k = 0, set

$$\hat{x}_0 = E(x_0) \quad (8)$$

$$P_{(0)} = E\left[(x_0 - \hat{x}_0)(x_0 - \hat{x}_0)^T\right] \quad (9)$$

Step 2 Computation: For k = 1,2,3,…, compute
Time update:

$$\hat{x}_{k/k-1} = A_{k-1}\hat{x}_{k-1} + B_{k-1}u_{k-1} \quad (10)$$

$$P_{k/k-1} = A_{k-1}P_{k-1}A_{k-1}^T + \Gamma_{k,k-1}Q\Gamma_{k,k-1}^T \quad (11)$$

Kalman gain:

$$K_k = P_{k/k-1}C_k^T\left(C_kP_{k/k-1}C_k^T + R\right)^{-1} \quad (12)$$

Measurement update:

$$\hat{x}_{k/k} = \hat{x}_{k/k-1} + K_k\left[z_k - h\left(\hat{x}_{k/k-1}, u_k\right)\right] \quad (13)$$

$$P_k = (I - K_kC_k)P_{k/k-1} \quad (14)$$

Table 3
Summary of UKF algorithm.

The state equation and the observation equation of the nonlinear discrete system

$$\begin{cases} x_k = f(x_{k-1}, u_{k-1}) + \omega_{k-1} \\ z_k = h(x_k, u_k) + v_k \end{cases} \quad (15)$$

Initialization: For k = 0, set

$$\begin{cases} \widehat{x}_{(0)} = \mathbf{E}\left(x_{(0)}\right) \\ \mathbf{P}_{(0)} = \mathbf{E}\left[\left(x_{(0)} - \widehat{x}_{(0)}\right)\left(x_{(0)} - \widehat{x}_{(0)}\right)^T\right] \end{cases} \quad (16)$$

The first sigma point selection

$$\begin{cases} \xi_{0,k} = \widehat{x}_{k-1} \\ \xi_{i,k} = \widehat{x}_{k-1} + \left(\sqrt{(n+k)\mathbf{P}_{k-1}}\right)^T \\ \xi_{i+n,k} = \widehat{x}_{k-1} - \left(\sqrt{(n+k)\mathbf{P}_{k-1}}\right)^T \end{cases} \quad (17)$$

Weight calculation

$$\begin{cases} w_i = \begin{cases} \lambda/(n+\lambda), i = 0 \\ 1/2(n+\lambda), i \neq 0 \end{cases} \\ w_i = \begin{cases} \lambda/(n+\lambda) + 1 + \beta - \alpha^2, i = 0 \\ 1/2(n+\lambda), i \neq 0 \end{cases} \\ \lambda = \alpha^2(n+k) - n \end{cases} \quad (18)$$

Time update:

$$\begin{cases} r_{ik/k-1} = f_{k-1}(\xi_{i,k-1}) + q_{k-1} \\ \widehat{x}_{k/k-1} = \sum_{i=0}^{L} w_i^m r_{i,k/k-1} = \sum_{i=0}^{L} w_i^m f_{k-1}(\xi_{i,k-1}) + \omega_{k-1} \\ \mathbf{P}_{k/k-1} = \sum_{i=0}^{L} w_i^c \left(r_{i,k/k-1} - \widehat{x}_{k/k-1}\right)\left(r_{i,k/k-1} - \widehat{x}_{k/k-1}\right)^T + \mathbf{Q} \end{cases} \quad (19)$$

The second sigma point selection according to formula (4)
Then, the measurement update

$$\begin{cases} \theta_{i,k/k-1} = h_k(\xi_{i,k-1}) + r_k \\ \widehat{z}_{k/k-1} = \sum_{i=0}^{L} w_i^m \theta_{i,k-1} = \sum_{i=0}^{L} w_i^m h_k(\xi_{i,k-1}) + v_k \\ \mathbf{P}_{\widetilde{z}_k} = \sum_{i=0}^{L} w_i^c \left(\theta_{i,k/k-1} - \widehat{z}_{k/k-1}\right)\left(\theta_{i,k/k-1} - \widehat{z}_{k/k-1}\right)^T + \mathbf{R} \\ \mathbf{P}_{\widetilde{x}_k \widetilde{z}_k} = \sum_{i=0}^{L} w_i^c \left(\xi_{i,k/k-1} - \widehat{x}_{k/k-1}\right)\left(\theta_{i,k/k-1} - \widehat{z}_{k/k-1}\right)^T \end{cases} \quad (20)$$

After getting z_k again, the measurement filter is updated

$$\begin{cases} \widehat{x}_k = \widehat{x}_{k/k-1} + K_k\left(z_k - \widehat{z}_{k/k-1}\right) \\ K_k = \mathbf{P}_{\widetilde{x}_k \widetilde{z}_k} \mathbf{P}_{\widetilde{z}_k}^{-1} \\ \mathbf{P}_k = \mathbf{P}_{k/k-1} - K_k \mathbf{P}_{\widetilde{z}_k} K_k^T \end{cases} \quad (21)$$

matrix, $\mathbf{R}$ is the measurement noise covariance matrix, Γ is the noise input matrix, $\mathbf{P}$ is the covariance matrix, and $\mathbf{K}$ is the Kalman gain vector.

4.2. Use the DUKF algorithm to online estimate model parameters and SOC simultaneously

Due to the variability of the operating conditions of the electric vehicle, battery parameters can easily affected by the ambient factors, such as current, temperature and etc. Therefore, it is not advisable to combine the offline identification battery parameters with the improved SOC estimation algorithm. The online parameters identification method has many advantages compared with the offline identification: 1) it effectively avoids the time waste and the error of the parameters calibration resulted from the offline experiments; 2) the real time estimation of the battery parameters enables to eliminate the interference generated from the ambient factors. 3) It is helpful to online estimate the real time states by considering the time-varying characteristics of the parameters. In this study, an algorithm named DUKF is proposed to realize the online parameters identification and the SOC estimation simultaneously. And the application process is shown in Fig. 5.

The DUKF is carried out as: 1) input the initial values (the approximate initial values of the battery parameters need to be calculated according to formula (2) to (5)); 2) use the time update model parameters from the UKF 2 as the inputs to estimate the SOC, U_{P1} and U_{P2}; 3) use this above three state quantities as the known quantities to realize the model parameters identification; and 4) these two filters are iterated in real time, and the battery parameters and states are estimated simultaneously. In Fig. 6, the UKF l algorithm achieves the estimation of the battery SOC, U_{P1} and U_{P2} and the specific calculation process is on the basis of formula (22) to (23). The specific formula of UKF 2 is mainly according to equation (24). The DUKF algorithm effectively reduces the dimension of parameters needed to estimate and make the equations more effective.

The definition equation for the state of charge is:

$$SOC = SOC_0 - \frac{\int \eta i(t)dt}{C_{cell}} \quad (22)$$

where the η is the charge/discharge rate, SOC_0 is the initial value of the SOC, C_{cell} is the nominal capacity of the battery.

The state equation of the UKF1 is as follows:

$$\begin{cases} \begin{bmatrix} U_{p1,k} \\ U_{p2,k} \\ SOC_k \end{bmatrix} = \begin{bmatrix} e^{-T_S/C_{P1,k-1}R_{P1,k-1}} & 0 & 0 \\ 0 & e^{-T_S/C_{P2,k-1}R_{P2,k-1}} & 0 \\ 0 & 0 & 1 \end{bmatrix} \begin{bmatrix} U_{p1,k-1} \\ U_{p2,k-1} \\ SOC_{k-1} \end{bmatrix} + \begin{bmatrix} R_{p1}\left(1 - e^{-T_S/C_{P1,k-1}R_{P1,k-1}}\right) \\ R_{p2}\left(1 - e^{-T_S/C_{P2,k-1}R_{P2,k-1}}\right) \\ -\dfrac{\eta T_S}{C_{cell}} \end{bmatrix} [i_{k-1}] + \omega_k \\ \\ [U_{L,k}] = \begin{bmatrix} -1 & -1 & 0 \end{bmatrix} \begin{bmatrix} U_{p1,k} \\ U_{p2,k} \\ SOC_k \end{bmatrix} - [R_{0_k}][i_k] + [U_{ocv}(SOC_k)] + v_k \end{cases} \quad (23)$$
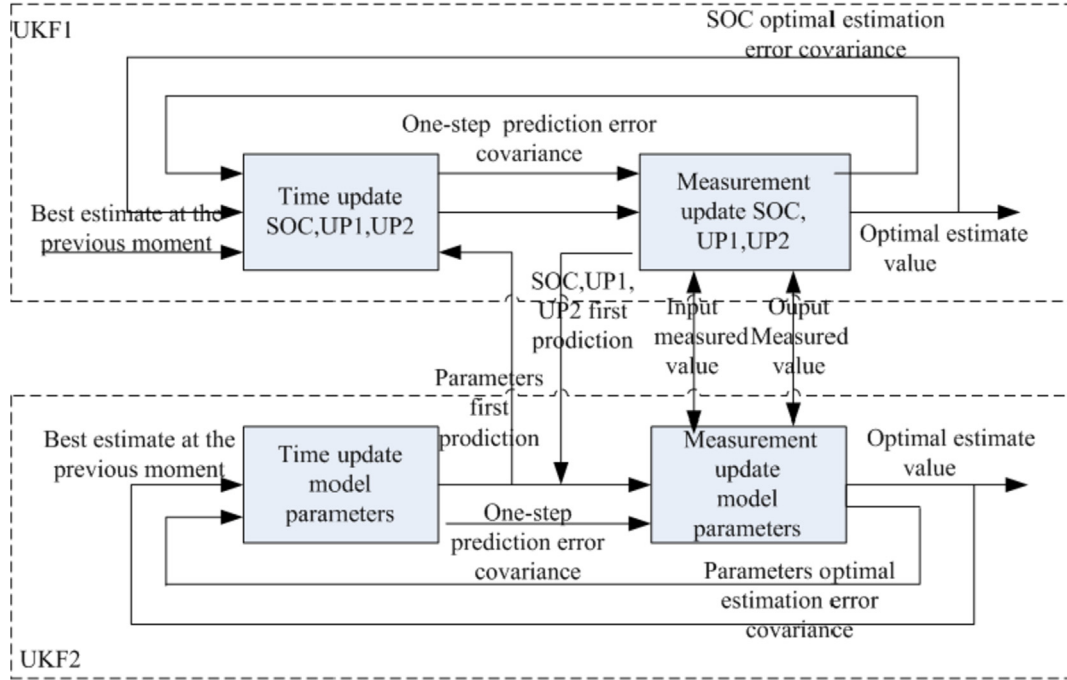
Fig. 5. A block diagram of battery parameters and SOC estimation algorithm based on DUKF.
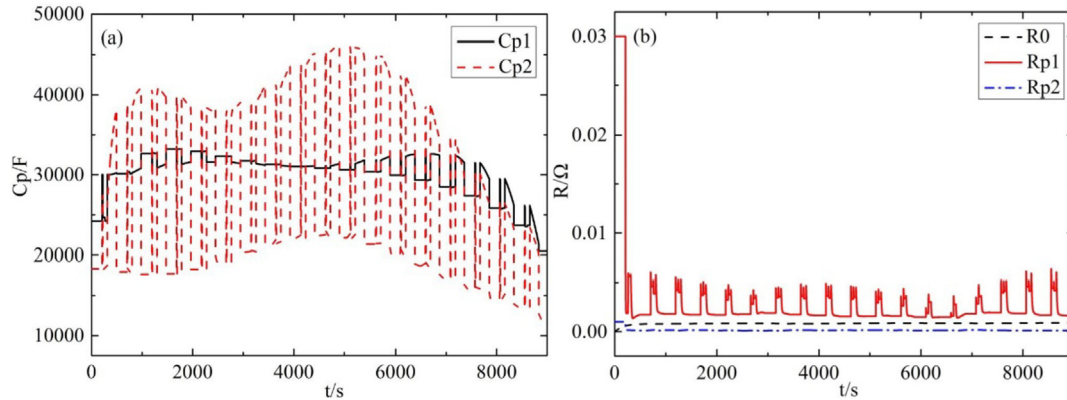

Fig. 6. Parameters identification results on the basis of DUKF algorithm.

T_s is the sampling period, ω_k is the system noise, v_k is the observation noise. The parameters are identified on the basis of offline parameters identification method. Here the $X_k = [U_{p1,k}, U_{p2,k}, SOC_k]^T$, $z_k = U_{L,k}$, and an online SOC estimation is carried out in accordance with formula (15)–(21).

In UKF2, the R_0, R_{p1}, C_{p1}, R_{p2}, C_{p2} are used as the parameters vector and they are considered to be slowly changing. And the specific equation defined as follows:

$$\theta_k = \theta_{k-1} + \gamma$$
$$U_{p1,k} = e^{-T_s/C_{P1,k-1}R_{P1,k-1}} U_{p1,k-1} + R_{p1}\left(1 - e^{-T_s/C_{P1,k-1}R_{P1,k-1}}\right) i_{k-1} + v_{1,k}$$
$$U_{p2,k} = e^{-T_s/C_{P2,k-1}R_{P2,k-1}} U_{p2,k-1} + R_{p2}\left(1 - e^{-T_s/C_{P2,k-1}R_{P2,k-1}}\right) i_{k-1} + v_{2,k}$$
$$U_{L,k} - U_{ocv}(SOC_{k-1}) - U_{p1,k} - U_{p2,k} = i_{k-1}R_0 + v_{3,k}$$

$$(24)$$

The $X_k = \theta_k = [R_{0_k}, R_{p1_k}, C_{p1_k}, R_{p2_k}, C_{p2_k}]^T$, γ_k is the small disturbance of the parameters, $\omega_k = \gamma_k$. $v_{1,k}, v_{2,k}, v_{3,k}$ represent for the observation noise. The z_k mainly consist of three parts: $U_{p1,k}$ is used

to observe the polarization parameters R_{p1} and C_{p1}; $U_{p1,k}$ served to observe the polarization parameters R_{p2} and C_{p2}; $U_{L,k} - U_{ocv}(SOC_{k-1}) - U_{p1,k} - U_{p2,k}$ is the observed variable of R_0. γ_k is the small disturbance of the parameters. The parameters identification is carried out in accordance with formula (15)–(21).

5. Results and discussion

5.1. Parameters identification

The DUKF algorithm is employed in this study to execute the online identification of parameters. The parameters identification results under the HPPC test is shown in Fig. 6. Fig. 6 (a) displays the polarization capacitance identification curves and Fig. 6 (b) shows the identification results of the ohimic resistance and the two polarization resistances.
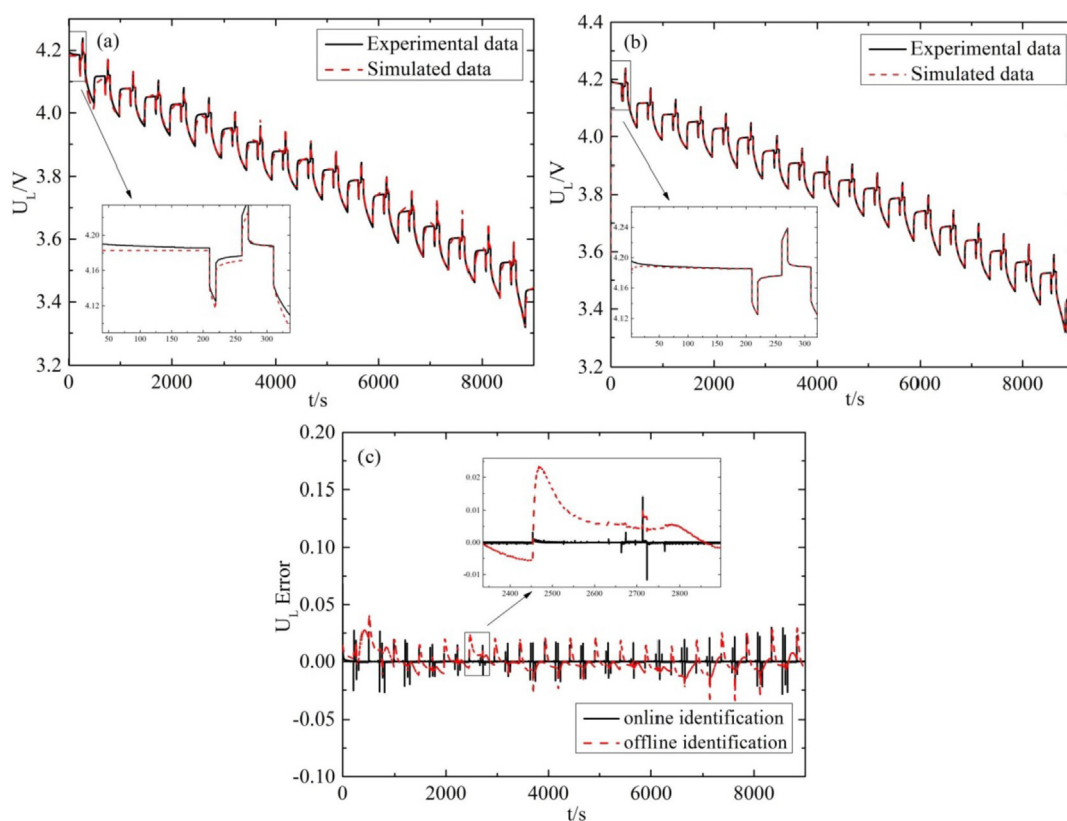
The comparison of the terminal voltage between the measurement and the simulation under the HPPC test is shown in Fig. 7 to illustrate accuracy and reliability of the online parameters

identification results on the basis of the DUKF algorithm. The red line in Fig. 7 (a) and (b) is the simulated terminal voltage on the basis of offline and online identification results, respectively. It is concluded from the plots that except the initial error caused by the setting of the initial value, the simulated data quickly converges to the experimental data, making a good response during the whole process. Therefore, the method is proved to be feasible and reliable. Fig. 7 (c) shows the comparison of the model error on the basis of two different parameters identification results. It is found that in the majority cases the error of the online identification is highly lower than that of the offline identification except some local points. As a whole, it has higher precision and corresponding ability on the basis of DUKF algorithm under the HPPC test.

Fig. 8 (a) to (b) displays the distribution of the model errors under the online and offline identification. The two errors are basically treated as obeying the Gauss distribution. The standard deviation is often used as a measure of the degree of statistical distribution, reflecting the degree of dispersion between individuals within the group. From the comparison, it is concluded that the frequency distribution of the online identification is relatively more concentrated. In Fig. 8 (a), the mean error is very close to zero and the standard deviation is also very small, reflecting that the entire error is concentrated at a very small level. In Fig. 8 (b), the degree of concentration is lower and the average error is higher. Therefore, it is proved that the online parameters identification method shows obviously the advantage of high precision.

Fig. 9 (a) to (b) show the online parameters identification results on the basis of the DUKF algorithm under the DST test. In Fig. 9 (a),
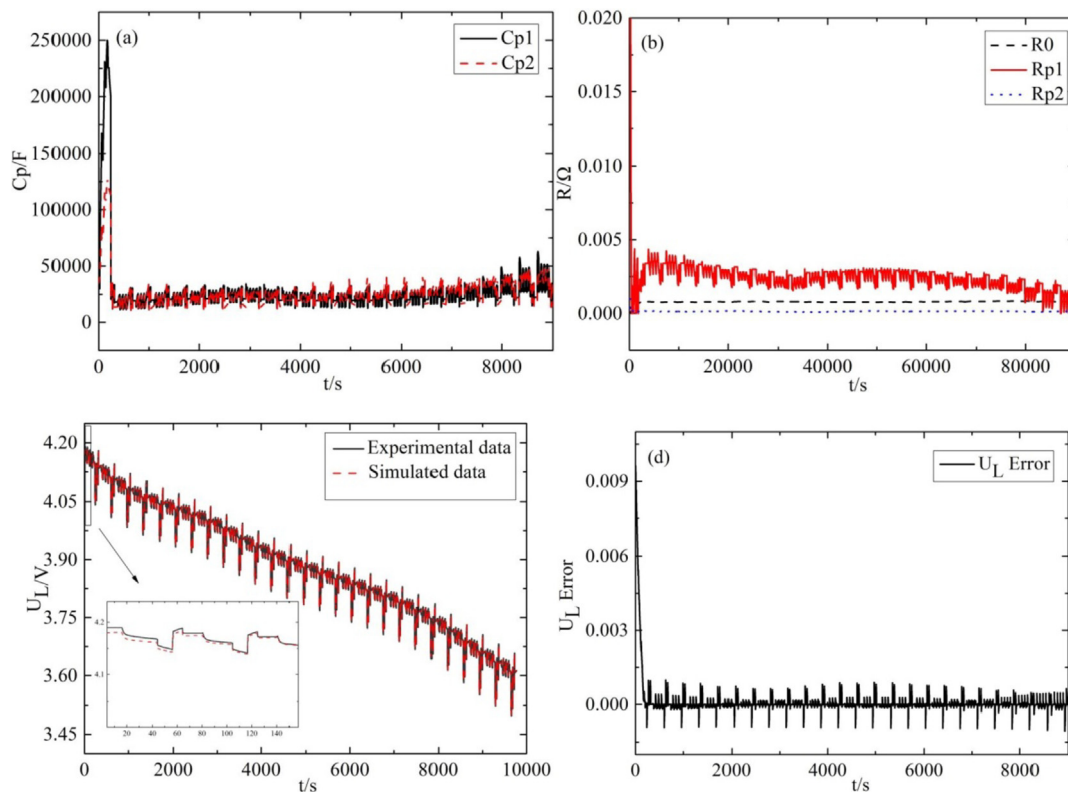

Fig. 7. (a) The comparison of the terminal voltage between the experimental and the simulated data under the offline identification; (b) The comparison of the terminal voltage between the experimental and the simulated data under the online identification; (c) The comparison of the terminal voltage error under the offline identification and the online identification.
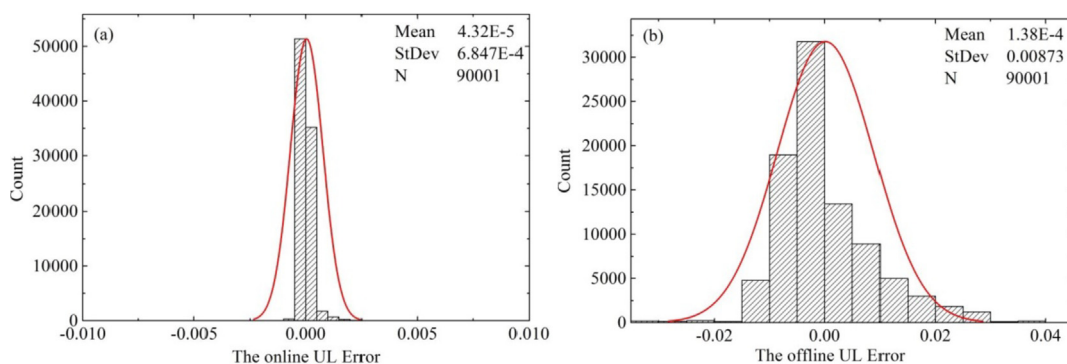
Fig. 8. Error distribution under the HPPC test, (a) the model error distribution on the basis of the online parameters identification; (b) the model error distribution on the basis of the offline parameters identification.

Fig. 9. (a) The polarization capacitance identification results under the DST test; (b) The polarization resistance and the internal resistance identification results under the DST test; (c) The comparison of the experimental terminal voltage and the simulated terminal voltage under the DST test; (d) The terminal voltage error under the DST test.

after applying the current, C_{p1} and C_{p2} show the trend of rising rapidly to the peak and then decreased rapidly in a short period of time. In addition, these two parameters all rebounded slightly at the end of discharge under the DST test. In Fig. 9 (b), the values of these two polarization resistances show obvious differences because of different polarization reaction rates. The online identification of polarization parameters not only avoids the repetition of calibration parameters, but also corrects the noise measuring drift due to the external factors, realizing the accurate prediction of each state on the basis of DUKF algorithm. To illustrate the accuracy and reliability of the online parameters identification results, the comparison between the experimental and the simulated terminal voltage under the DST test is shown in Fig. 8(c) to (d). It is seen from the plots that the simulation quickly converges to the measurement and makes a good response during the whole process. Therefore, it is proved that this method is feasible and reliable.

It is emphasized that the parameters of the online identification enable the SOH estimation to be realized online. Normally, it is defined that the 200% of the initial battery internal resistance as the end of life (EOL) [26]. In addition, the definition of SOH based on internal resistance estimator is as follows:

$$SOH = \frac{R_{0\_EOL} - R_{0\_now}}{R_{0\_EOL} - R_{0\_new}} \times 100\% \tag{25}$$

R_{0_now} is the ohmic resistance of the battery in the current state, R_{0_new} is the ohmic resistance of the battery in the initial state, R_{0_EOL} is the ohmic resistance of the battery to the aging state.

From Figs. 7–9, it is proved that the online identification of resistances is realized effectively on the basis of DUKF algorithm under the HPPC test and DST test, respectively. Fig. 10 shows the

online identification of R_0 under the DST test, changing with SOC that is a varied parameter under the actual operating condition. Therefore, it is necessary to estimate SOC at the same time when using R_0 to characterize the battery SOH. The validation of the online SOH estimation will be studied in our further work, which is beyond this study.

In conclusion, on the basis of the DUKF algorithm, the terminal voltage error is highly lower of the online identification than of the offline identification and the error distribution of the online identification is relatively more concentrated under the HPPC test. Besides, the simulation quickly converges to the measurement and makes a good response during the whole DST test.

5.2. SOC estimation

Fig. 11 is SOC estimation on the basis of three different algorithms, the EKF algorithm, the UKF algorithm and the DUKF algorithm. Fig. 11 (a), (c) and (e) show the SOC estimation on the basis of three algorithms under the constant current discharge test, HPPC test and DST test. Fig. 11 (b), (d) and (f) provide the corresponding errors of the estimation.

Under the constant current discharge test and DST test, the convergence speed of the SOC estimation under the EKF algorithm is the slowest, whereas the convergence speed of the results under the UKF and DUKF algorithm is almost the same. The accuracy of the SOC estimation result under the DUKF is the highest. Under the HPPC test, the SOC estimation under the EKF and the DUKF shows the slowest and the fast convergence speed, respectively. The accuracy of the estimation under the DUKF is the highest, whereas the accuracy under the EKF and the UKF is quite unobvious. From Fig. 11, it is concluded that the SOC estimation on the basis of DUKF
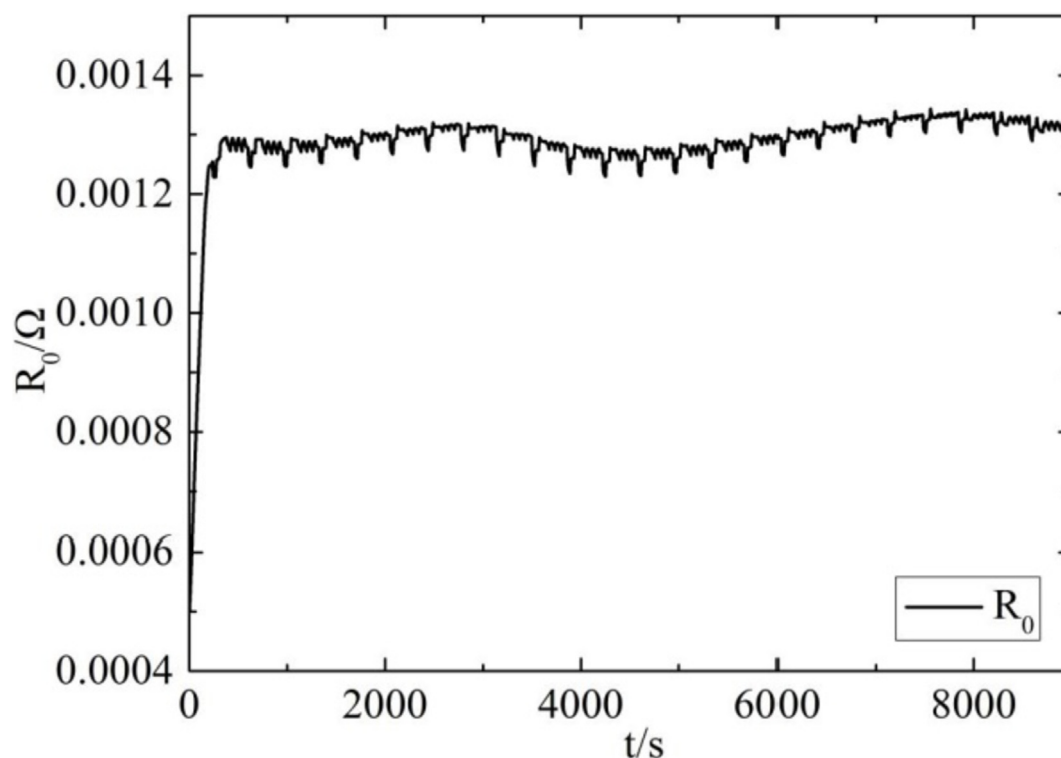
Fig. 10. The online identification of the internal resistance under the DST test.

algorithms has both the best dynamic performance and the minimum error.

In Table 4, the accuracy of SOC estimation is analyzed in terms of the maximum error, the mean error, the RMSE (the root mean square error) and the convergence time. The real SOC starts from 100% while the initial value of the simulation is 20%. The convergence time is defined as the range from the initial time to the time when the SOC difference between the simulation and the measurement is less than 1%. The less the convergence time, the stronger dynamic following ability this algorithm has. The results of three algorithms under the CCD, HPPC, and DST test are listed in Table 4, respectively. From the comparison of different operating conditions, almost all of the statistical errors are minimal under the DST test. Besides, the convergence time is the fastest under the DST test. These results explain that all models exhibit good dynamic performance, representing that the algorithms based on Kalman Filter are adapted to be applied in dynamic operating conditions. Compared with the SOC estimation errors on the basis of the EKF, UKF and DUKF algorithm, the results show that the convergence speed is obviously lower of the EKF algorithm than others. The comparison of the accuracy also shows that EKF is obviously the lowest. The facts are explained as EKF only achieves the first order accuracy, whereas other two algorithms have the second order accuracy. Furthermore, the accuracy is higher of DUKF than UKF due to the online parameter identification realized by the former.

Taking the practical application of electric vehicles into consideration, the different input values of SOC are chosen as the starting point. The input SOC is set at 0.2, 0.4, 0.6 and 0.8, respectively. It is seen from the Fig. 12 that even if there is an error in the initial value, simulation quickly converges to the real SOC. From the local enlarged plot, the simulated curves spend about 40, 70, 80 and

90 s convergence to approach the real one when the input value is set at 0.8, 0.6, 0.4 and 0.2, respectively. Moreover, the difference is small between the every two convergent curves, and after 100 s the SOC estimation error is less than 2% even if the initial error is maximum. Therefore, the proposed algorithm has good robustness and accuracy.

In conclusion, from the comparison of different operating conditions, the maximum error, the mean error and the RMSE of the SOC estimation are less under DUKF algorithm than under the EKF and UKF algorithm. Moreover, it is proved that the under the DUKF algorithm, the simulation curve is insensitive to the initial error and quickly converges to the real value.

6. Conclusion

By studying a large amount of literature, we propose a superior algorithm named dual unscented Kalman filter to simultaneously realize the online identification of parameters and estimation of SOC. The main conclusions are drawn as following:

(1) Except U_{OCV}, all parameters concluding R_0, R_{p1}, C_{p1}, R_{p2} and C_{p2} in the DP model are fulfilled online identification by using DUKF, along with the online estimation of SOC and SOH. Note that different from a resistance and a capacitance, U_{ocv} represents the thermodynamic performance of the battery, which is generally obtained by measurement.

(2) The error of the online parameters identification results on the basis of DUKF algorithm is highly lower than that of the offline identification and the error distribution of the online identification is relatively more concentrated. Under the DST
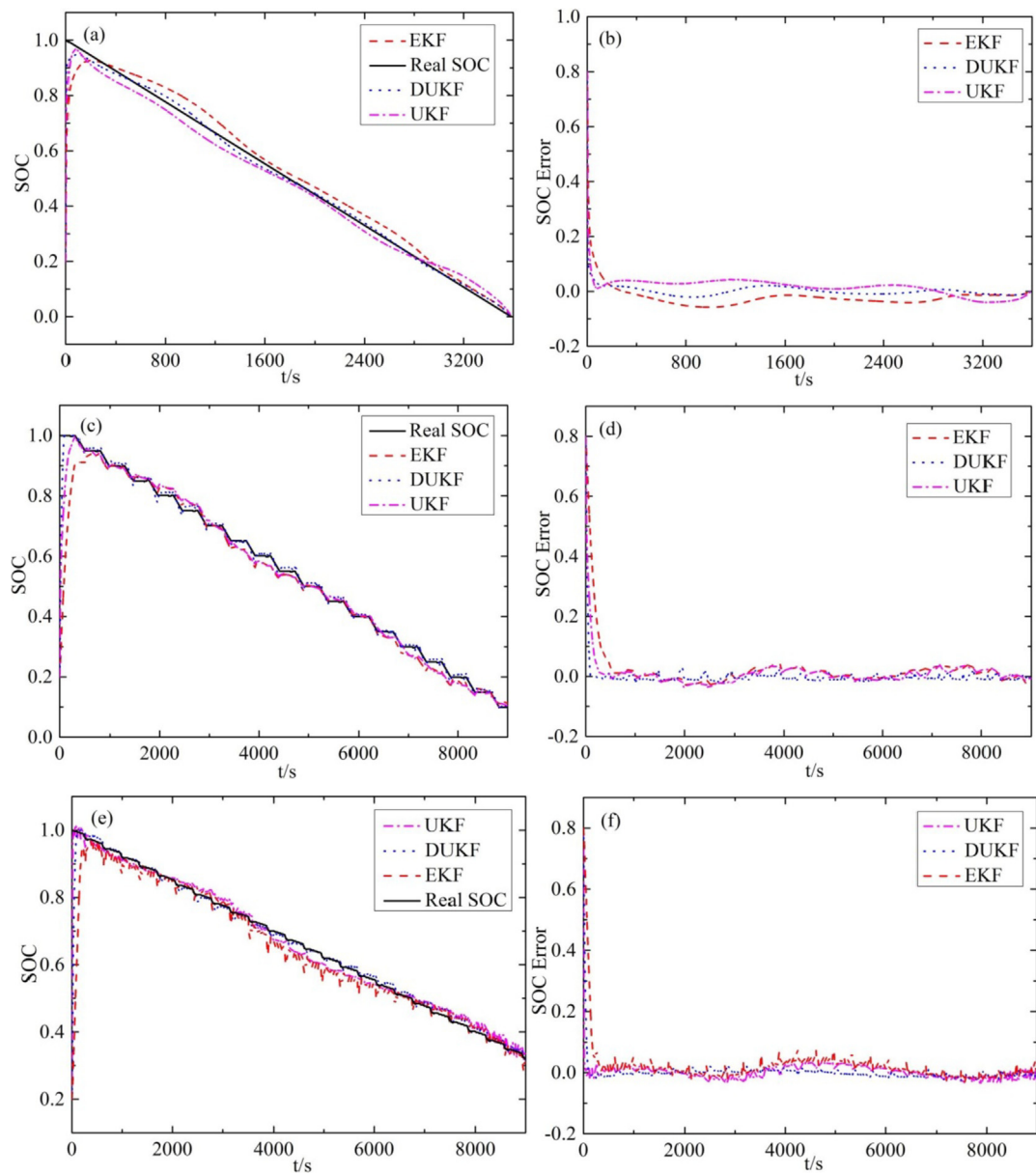
Fig. 11. (a)The SOC estimation results under the constant current discharge test; (b)The SOC estimation error under the constant current discharge test; (c)The SOC estimation results under the HPPC test; (d)The SOC estimation error under the HPPC test; (e)The SOC estimation results under the DST test; (f)The SOC estimation error under the DST test.

Table 4
SOC estimation errors analysis under different algorithms.

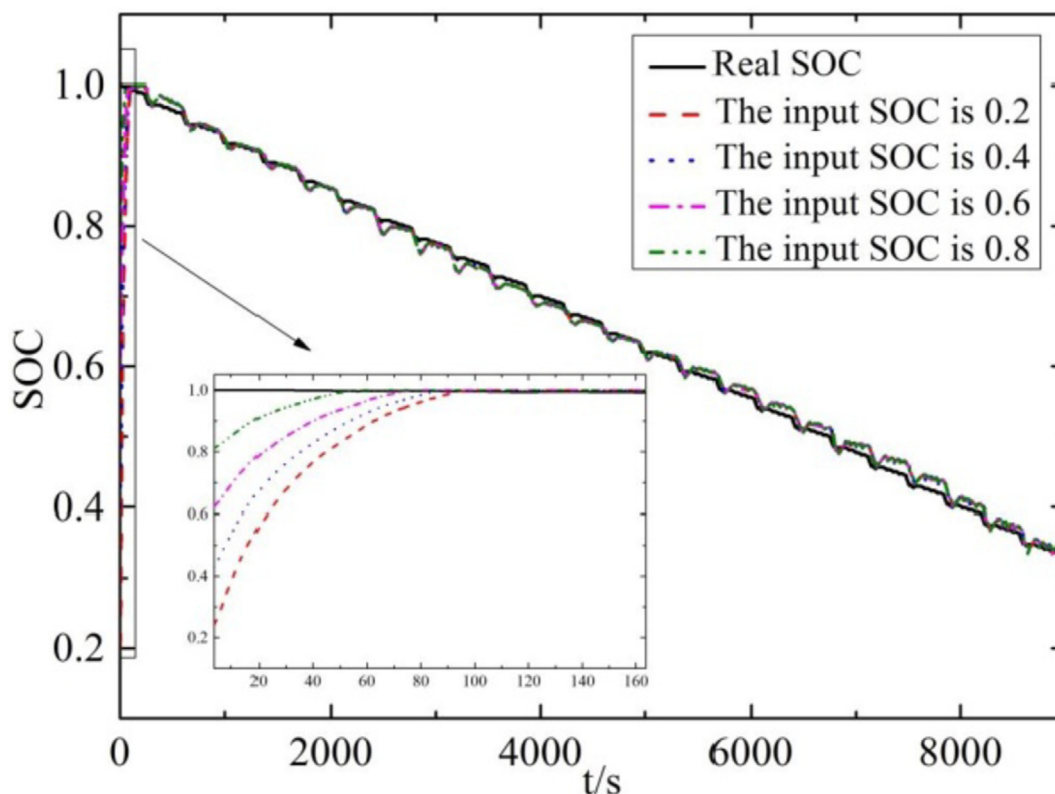| Operating Conditions	Algorithm	Maximum	Mean	RMSE	Convergence Time/s
CCD Test	EKF	0.05374	0.01183	0.01428	445
	UKF	0.04753	0.00972	0.01029	108
	DUKF	0.02048	0.00431	0.00694	103
HPPC Test	EKF	0.03158	0.00815	0.00993	378
	UKF	0.02976	0.00794	0.00874	137
	DUKF	0.01573	0.00352	0.00472	98
DST Test	EKF	0.03146	0.00732	0.00833	226
	UKF	0.02838	0.00571	0.00691	88
	DUKF	0.01152	0.00294	0.00338	90

Fig. 12. The SOC estimation with different input values under the DST test.

test, it is proved that the parameter identification have both the good dynamic performance and high precision.

(3) The SOC estimation is verified by the CCD, HPPC and DST test. The converge speed of the SOC estimation under the DUKF is less than 103 s, which is as quickly as under the UKF algorithm, but faster than EKF. The maximum SOC estimation error under the DUKF algorithm is kept within 3%, less than the error under the EKF and UKF algorithm, and showing a high precision.

Acknowledgement

References

[1] J.A.P. Lopes, F.J. Soares, P.M.R. Almeida, Integration of electric vehicles in the electric power system, Proc. IEEE 99 (2011) 168—183.
[2] A. Zenati, P. Desprez, H. Razik, Estimation of the SOC and the SOH of li-ion batteries, by combining impedance measurements with the fuzzy logic inference, in: IECON 2010-36th Annual Conference on IEEE Industrial Electronics Society, 2010, pp. 1773—1778.
[3] N. Yang, X. Zhang, G. Li, State of charge estimation for pulse discharge of a LiFePO4 battery by a revised Ah counting, Electrochim. Acta 151 (2015) 63—71.
[4] Y. Xing, W. He, M. Pecht, K.L. Tsui, State of charge estimation of lithium-ion batteries using the open-circuit voltage at various ambient temperatures, Appl. Energy 113 (2014) 106—115.
[5] Y.H. Chiang, W.Y. Sean, J.C. Ke, Online estimation of internal resistance and open-circuit voltage of lithium-ion batteries in electric vehicles, J. Power Sources 196 (2011) 3921—3932.
[6] M. Charkhgard, M. Farrokhi, State-of-Charge estimation for lithium-ion batteries using neural networks and EKF, IEEE Trans. Ind. Electron. 57 (2010) 4178—4187.
[7] C.H. Piao, W.L. Fu, W. Jin, Z.Y. Huang, C. Cho, Estimation of the state of charge of Ni-MH battery pack based on artificial neural network, in: INTELEC 2009-31st International Telecommunications Energy Conference, 2009, pp. 1—4.
[8] L. Zhong, C. Zhang, Y. He, Z. Chen, A method for the estimation of the battery pack state of charge based on in-pack cells uniformity analysis, Appl. Energy 113 (2014) 558—564.
[9] Y. Wang, C. Zhang, Z. Chen, A method for state-of-charge estimation of LiFePO4 batteries at dynamic currents and temperatures using particle filter, J. Power Sources 279 (2015) 306—311.
[10] P. Spagnol, S. Rossi, S.M. Savaresi, Kalman filter SoC estimation for Li-Ion batteries, in: 2011 IEEE International Conference on Control Applications (CCA), 2011, pp. 587—592.
[11] D.D. Domenico, G. Fiengo, A. Stefanopoulou, Lithium-ion battery state of charge estimation with a Kalman Filter based on a electrochemical model, in: 2008 IEEE International Conference on Control Applications, 2008, pp. 702—707.
[12] C. Hu, B.D. Youn, J.A. Chung, Multiscale framework with extended Kalman filter for lithium-ion battery SOC and capacity estimation, Appl. Energy 92 (2012) 694—704.
[13] S. Sepasi, R. Ghorbani, B.Y. Liaw, A novel on-board state-of-charge estimation method for aged Li-ion batteries based on model adaptive extended Kalman filter, J. Power Sources 245 (2014) 337—344.
[14] R. Xiong, H. He, F. Sun, K. Zhao, Evaluation on state of charge estimation of batteries with adaptive extended Kalman filter by experiment approach, IEEE Trans. Veh. Technol. 62 (2013) 108—117.
[15] C.H. Tong, T.D. Barfoot, A comparison of the EKF, SPKF, and the Bayes filter for landmark-based localization, in: 2010 Canadian Conference on Computer and Robot Vision, 2010, pp. 199—206.
[16] J.L. Zhang, Battery state-of-charge estimation based on sigma point Kalman filter, in: 2011 2nd International Conference on Artificial Intelligence, Management Science and Electronic Commerce (AIMSEC), 2011, pp. 3816—3819.
[17] Z. He, Y. Liu, M. Gao, W. Caisheng, A joint model and SOC estimation method for lithium battery based on the sigma point KF, in: 2012 IEEE Transportation Electrification Conference and Expo (ITEC), 2012, pp. 1—5.
[18] Y. Tian, Z. Chen, F. Yin, Distributed IMM-unscented Kalman filter for speaker tracking in microphone array networks, in: IEEE/ACM Transactions on Audio, Speech, and Language Processing, vol. 23, 2015, pp. 1637—1647.
[19] G.L. Plett, Extended Kalman filtering for battery management systems of LiPB-based HEV battery packs, Part 3. State and parameter estimation, J. Power Sources 134 (2004) 277—292.
[20] H. Mahdianfar, A. Pavlov, O.M. Aamo, Joint unscented Kalman filter for state and parameter estimation in managed pressure drilling, in: 2013 European Control Conference (ECC), 2013, pp. 1645—1650.
[21] G L Plett. Method and system for joint battery state and parameter estimation: U.S. Patent 7,593,821. 2009-9—22.
[22] M.E. Gharamti, B. Ait-El-Fquih, I. Hoteit, A one-step-ahead smoothing-based joint ensemble Kalman filter for state-parameter estimation of hydrological

models, in: S. Ravela, A. Sandu (Eds.), Dynamic Data-driven Environmental Systems Science: First International Conference, DyDESS 2014, Cambridge, MA, USA, November 5-7, 2014, Revised Selected Papers. Cham: Springer International Publishing, 2015, pp. 207—214.

[23] T.A. Wenzel, B.K.J. urnham, M.V. Blundell, R.A. Williams, Dual extended Kalman filter for vehicle state and parameter estimation, Veh. Syst. Dyn. 44 (2006) 53—171.

[24] S. Lee, J. Kim, J. Lee, B. Cho, State-of-charge and capacity estimation of lithium-ion battery using a new open-circuit voltage versus state-of-charge, J. Power Sources 185 (2008) 1367—1373.

[25] C. Chen, F. Sun, R. Xiong, H.W. He, A novel dual H infinity filters based battery parameter and state estimation approach for electric vehicles application, Energy Proc. 103 (2016) 375—380.

[26] D. Andre, C. Appel, T. Soczka-Guth, D.U. Sauer, Advanced mathematical methods of SOC and SOH estimation for lithium-ion batteries, J. Power Sources 224 (2013) 20—27.

[27] H. Dai, Wei, Z. Sun, J. Wang, W. Gu, Online cell SOC estimation of Li-ion battery packs using a dual time-scale Kalman filtering for EV applications, Appl. Energy 95 (2012) 227—237.

[28] R. Xiong, F. Sun, Z. Chen, H. He, A data-driven multi-scale extended Kalman filtering based parameter and state estimation approach of lithium-ion olymer battery in electric vehicles, Appl. Energy 113 (2014) 463—476.

[29] X. Shen, T. Shen, X. Zha, K. Hikiri, State-of-charge estimation of super-capacitor using dual extended Kalman filter, in: Proceedings of the 33rd Chinese Control Conference, 2014, pp. 227—232.

[30] X. Zhang, Y. Wang, D. Yang, Z. Chen, An on-line estimation of battery pack parameters and state-of-charge using dual filters based on pack model, Energy 115 (2016) 219—229.

[31] Y. Wang, J.C. Principe, Tracking the non-stationary neuron tuning by dual Kalman filter for brain machine interfaces decoding, in: 2008 30th Annual International Conference of the IEEE Engineering in Medicine and Biology Society, 2008, pp. 1720—1723.

[32] J. Kim, B.H. Cho, State-of-Charge estimation and state-of-health prediction of a Li-Ion degraded battery based on an EKF combined with a per-unit system, IEEE Trans. Veh. Technol. 60 (2011) 4249—4260.

[33] B.S. Bhangu, P. Bentley, D.A. Stone, C.M. Bingham, Nonlinear observers for predicting state-of-charge and state-of-health of lead-acid batteries for hybrid-electric vehicles, IEEE Trans. Veh. Technol. 54 (2005) 783—794.

[34] US Department of Energy, PNGV Battery Test Manual, INEEL, Washington D C, 2001-02.

[35] US Department of Energy, USABC Electric Vehicle Battery Test Procedure Manual, USABC, Washington D C, 1996-01.

[36] Q. Wang, J. Wang, P. Zhao, J. Kang, F. Yan, C. Du, Correlation between the model accuracy and model-based SOC estimation, Electrochim. Acta 228 (2017) 146—159.

[37] J. Kang, F. Yan, P. Zhang, C. Du, A novel way to calculate energy efficiency for rechargeable batteries, J. Power Sources 206 (2012) 310—314.

[38] S.J. Julier, J.K. Uhlmann, Unscented filtering and nonlinear estimation, Proc. IEEE 92 (2004) 401—422.

[39] Q.T. Wang, Y.Z. Jiang, Y.H. Lu, State of health estimation for lithium-ion battery based on D-UKF, Int. J. Hybrid Inf. Technol. 8 (2015) 55—70.